

**OMAE2020-18171**

**DRAFT: EFFECT OF A PASSIVE TUNED MASS DAMPER ON OFFSHORE  
INSTALLATION OF A WIND TURBINE NACELLE**

**Zhiyu Jiang**

Department of Engineering Sciences  
University of Agder  
N-4879 Grimstad, Norway  
[zhiyu.jiang@uia.no](mailto:zhiyu.jiang@uia.no)

**Trond Kvaa Skrudland**

Department of Engineering Sciences  
University of Agder  
N-4879 Grimstad, Norway  
[trond-ks@hotmail.com](mailto:trond-ks@hotmail.com)

**Madjid Karimirad**

School of Natural and Built  
Environment  
Queen's University Belfast, UK  
[madjid.karimirad@qub.ac.uk](mailto:madjid.karimirad@qub.ac.uk)

**Constatine Machiladies**

Department of Civil Engineering and  
Geomatics  
Cyprus University of Technology  
Limassol 3036, Cyprus  
[c.michailides@cut.ac.cy](mailto:c.michailides@cut.ac.cy)

**Wei Shi**

Deepwater Engineering Research  
Center  
Dalian University of Technology  
116024 Dalian, China  
[weishi@dlut.edu.cn](mailto:weishi@dlut.edu.cn)

**ABSTRACT**

Although the installation of offshore wind turbines takes place in calm seas, successful mating of wind turbine components can be challenging due to the relative motions between the two mating parts. This work investigates the effect of a passive tuned mass damper on the mating processes of a nacelle for a 10-megawatt (MW) offshore wind turbine. A nacelle with lifting wires and a monopile with a mass damper are respectively modelled using the multibody formulation in the HAWC2 program. A single mass damper is tuned to target at the first natural period of the monopile and is coupled to the main program using a dynamic link library. Afterwards, numerical simulations were carried out in turbulent wind conditions and irregular wave conditions typical of offshore installation scenarios. Important response variables including the tower-top motions, nacelle motions, and their relative motions are examined in the analysis. By comparing the time series and response statistics, we found that the tower-top motion is more crucial to the installation process than the lifted nacelle motion. For the relative motions and velocities between the nacelle and the tower top, the tuned mass damper can reduce the short-term maximum values by more than 50% for

the examined sea states with spectral period between 4 to 12 seconds. This implies that the weather window for marine operations can be expanded if the tuned mass damper is applied.

**KEYWORDS**

Offshore wind turbines, crane operation, jack-up vessel, response-based criteria, contact/impact analysis, installation method

**INTRODUCTION**

The development of offshore wind energy industry has been gaining momentum in the past decade. In Europe alone, there is an average annual increase of 30% in terms of installed capacity, and installations in the UK and Germany accounted for most new additions [1].

The development of an offshore wind farm involves several phases; the installation phase can cost 5 to 15% of overall capital costs [2]. An offshore installation is a typical type of marine operation that faces challenges of installation

technologies, logistics, weather window, and safety. The installation technologies relate to the type of foundation and development of specialised vessels and equipment. For example, barges are often involved to transport monopile offshore wind turbines (OWTs), and floating crane vessels are used to install foundations. For installation of floating foundations, different methods exist. Jiang et al. [3] presented a catamaran installation vessel for installing a wind turbine assembly onto a cylindrical floating or bottom-fixed foundation.

Offshore installations are usually performed with the significant wave height of less than 2 m, and it is desirable to increase the weather window and to avoid any unexpected delays. This is particularly important when many OWTs in a farm are to be installed. To assess whether an installation can be successfully carried out in a weather condition with wind and waves, a good understanding of the physics involved is necessary. We need to know the installation procedures and the critical events and make a refined numerical model in order to obtain the dynamic responses of the system under external load effects. Then, a response-based assessment can follow. Wilson et al. [4] presented a methodology for such an assessment.

## INSTALLATION OF OFFSHORE WIND TURBINE COMPONENTS

A conventional offshore wind turbine has components like support structure, tower, blades, nacelle, and hub. Depending on the types of OWTs, site conditions and installation facilities, there exist different installation methods [5]. Although the total number of offshore lifts and installation time may vary case by case, a crane vessel is generally needed to lift the components. Special-purpose jack-up vessels are favoured as they can transport OWT components and provide a stable foundation during lifting operations.

Figure 1 illustrates two examples of offshore installations using jack-up vessels. Figure 1 (top) corresponds to a single-blade installation which is a method that lifts three blades individually. A few recent works have addressed challenges of blade motion [6], monopile motions [7] and impact risks [8, 9] associated with the offshore single-blade installation. Figure 1 (bottom) corresponds a nacelle installation where the onboard crane transfers the nacelle from the installation vessel onto the tower. Like the single-blade installations, a nacelle installation may have difficulties because of wind-induced motions of the nacelle and wave-induced motions of the monopile, and crew assistance is involved in order to align the nacelle and the tower top during the mating phase.

To constrain the nacelle motions in the air, tugger lines can be connected to the nacelle; see Figure 2, where the sling wires, and lift wire transfer the nacelle weight to a crane. Still, during the mating phase where the nacelle is to be aligned with the

tower, the tower motions can still be a concern. The tower motion is influenced by the damping and excitation forces on the monopile-tower system. As the soil damping can be around 1% of critical damping, resonant motions of such a system can be a potential issue especially at sea states with small wave periods [10]. Jiang [11] focused on a 5-MW OWT during single-blade installation and showed that a passive tuned mass damper (TMD) can be used to facilitate the final installation process at wave periods close to the first eigen period of the monopile structure. In the present work, the effect of a tuned mass damper on the installation of a 10-MW OWT nacelle will be investigated.



**Figure 1** Examples of offshore wind turbines during installation (top: single-blade installation; bottom: nacelle installation. source: A2SEA A/S)

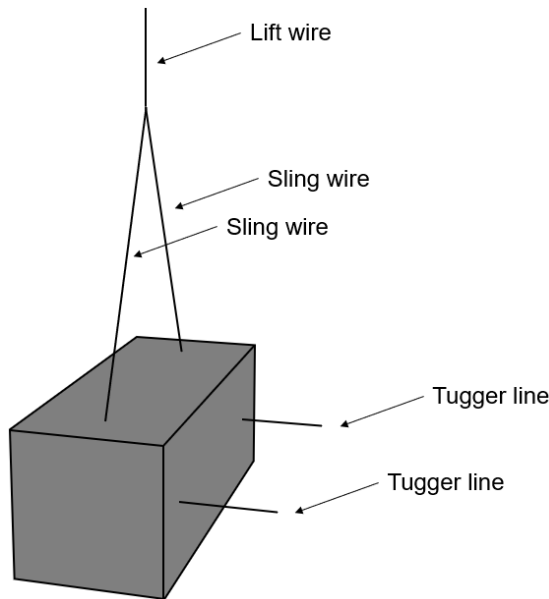


Figure 2 Illustration of a lifted nacelle with two tugger lines

## ANALYSIS PROCEDURE

This study presents a numerical analysis of the nacelle installation process of a 10-MW OWT. Figure 3 illustrates the analysis procedure. First, a representative lifted nacelle model and a monopile model with and without a TMD will be modelled using the multibody formulation [12]. Then, load cases are considered including decay tests and combined wind and wave cases. The decay tests are used to assess the damping characteristics of the monopile model, and the combined wind and wave cases to consider realistic environmental conditions for offshore nacelle installations. For the selected load cases, numerical simulations were carried out in the time domain, and response variables were obtained including the nacelle motions and the tower-top motions. Finally, post-processing was performed, and time series, response spectra, and response statistics are presented for evaluation of the TMD effect.

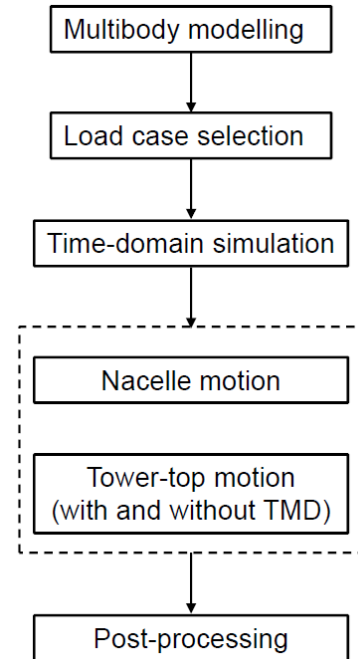


Figure 3 Flowchart of the present study

## NUMERICAL MODELLING

The numerical models for simulation of the OWT nacelle installation were established using HAWC2 [13], which is a state-of-the-art aeroelastic code. As the focus of this work is on the final stage prior to mating of the nacelle and the tower-top, the system is treated as a passive structure without active control. In the following, the structural, aerodynamic, and hydrodynamic modelling are respectively described.

### Structural modelling

The structural modelling of HAWC2 is based on multibody formulation [12]. The Timoshenko beam elements are used to model various parts of the installation system, and the parts are interconnected by coupling joints to allow large translations and rotations. Two subsystems are considered. The first subsystem is the nacelle model with lift wire, sling wires, and tugger lines. As shown in Figure 4, each cable is divided into five independent bodies and a ball bearing is used to allow relative rotation between the bodies and hence the noncompressible feature of the cables. Cable 2 and Cable 3 form an angle and a hook is expected at the connection point. One end of the cables is rigidly connected to the ground. This is a simplification that ignores the crane flexibility. The second subsystem is the preinstalled monopile and tower. The TMD is assumed to be installed inside the tower wall at the tower top. The interaction of the TMD system with the HAWC2 main program is achieved via an external dynamic link library so that the forces and moments of the TMD are feedback to the second subsystem

during time-domain simulations. Implementation and theory of the TMD can be found in [11, 14].

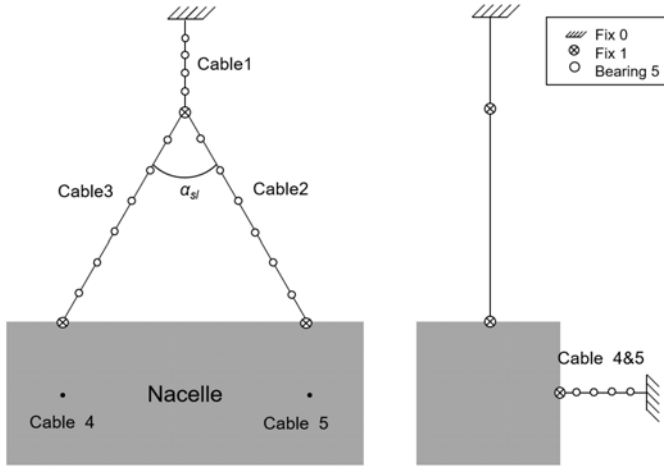


Figure 4 Schematic of the nacelle subsystem

### Aerodynamic loads

For the nacelle installation scenario, the aerodynamic loads are simplified. The steady drag and lift coefficients are used to determine the wind loads acting on each nacelle section. The crossflow principle [15] is applied during load calculation. This principle ignores the wind forces in the spanwise direction. For the tower, aerodynamic drag forces are applied, but these forces are negligible.

### Hydrodynamic loads

The Morison's formula is used to calculate the hydrodynamic loads on the monopile subsystem. For the monopile and the tower, the length is discretised into a few strips, and the unit hydrodynamic force normal to each strip is expressed as

$$f_z = \rho C_M \frac{\pi D^2}{4} \ddot{x}_w - \rho (C_M - 1) \frac{\pi D^2}{4} \dot{\eta}_1^2 + \frac{1}{2} \rho C_D D (\dot{x}_w - \dot{\eta}_1) |\dot{x}_w - \dot{\eta}_1| \quad (1)$$

where  $C_M$  and  $C_D$  respectively denote the mass and drag coefficients. The first and second derivative of  $x_w$  stand for the water particle velocity and acceleration, respectively, at the strip centre, and the first and second derivatives of  $\eta_1$  are the cylinder's velocity and acceleration. In Eq. (1), the first term includes the Froude-Kriloff and diffraction force, the second term is the inertial force, and the last term is the quadratic drag force [16].

## CASE STUDY

Here, the DTU 10-MW reference wind turbine [17] is selected. The two subsystems are sketched in Figure 5. For the first subsystem, as the dimension of the nacelle and cables are not specified, available information is considered of an MHI Vestas 10-MW OWT [18]. Parameters of the nacelle and the wires (Figure 4) are listed in Table 1. The monopile support structure utilised in this study is proposed by Velarde [19]. Basic properties of the monopile and the tower are listed in Table 2. Assuming a uniform sand layer, the lateral stiffness of the soil was extracted from finite element analysis and represented by  $p$ - $y$  curves in HAWC2. These curves can be found in [19].

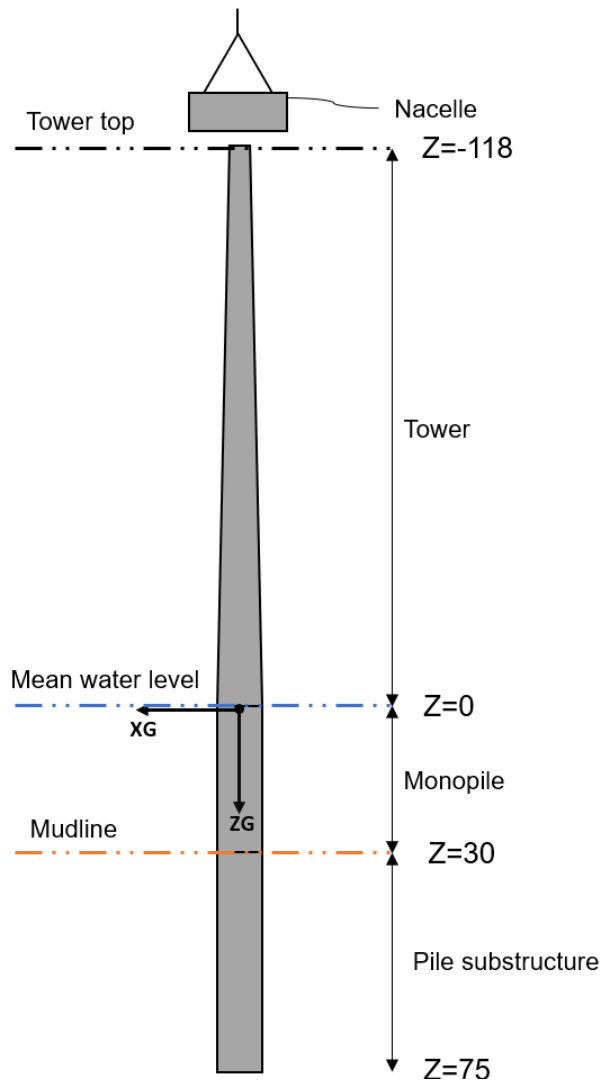


Figure 5 Illustration of the 10-MW monopile wind turbine during nacelle installation

Table 1 Key parameters of subsystem 1

Parameter	Notation	Value
Nacelle mass (tonnes)	$M_n$	446.0
Nacelle length (m)	$L_n$	20
Nacelle width (m)	$B_n$	8
Nacelle height (m)	$H_n$	8
Sling wire length (m)	$L_{sw}$	14
Lift wire length (m)	$L_{lw}$	5
Sling wire angle (deg)	$\alpha_{sl}$	60
Elastic modulus of wire (GPa)	$E$	210

Table 2 Key parameters of subsystem 2

Parameter	Notation	Value
Monopile diameter (m)	$D_m$	9
Pile penetration (m)	$P_m$	45
Monopile weight (tonnes)	$M_m$	1958.3
Transition piece weight (tonnes)	$M_{tp}$	500
Tower height (m)	$H_t$	118
Tower base diameter (m)	$D_{tb}$	9.5
Tower weight (tonnes)	$M_t$	628.4
First fore-aft natural period (s)	$t_{FA1}$	1.79

Table 3 List of the load cases in this study

LC	Category	$U_w$ (m/s)	$TI$	$H_s$ (m)	$T_p$ (s)
1	decay	-	-	-	-
2	wind/wave	6	0.20	1.0, 2.0	4, 8, 12
3	wind/wave	9	0.16	1.0, 2.0	4, 8, 12
4	wind/wave	12	0.14	1.0, 2.0	4, 8, 12

Table 3 lists the load cases considered. LC1 is the decay test where a constant force of 800 kN is applied at the monopile top for 200 seconds before the monopile experiences free decay without wind or waves. The free decay test only applies to the monopile subsystem. LC 2-4 are the wind and wave cases where the two subsystems are subjected to the combined load effects of wind and waves. Collinear wind and waves in the  $Y_G$ -direction (Figure 5) are considered. These environmental conditions are selected to reflect industrial practices. In LC 2-4, ten 1000-second simulations with random seed numbers were carried with and without the TMD. The first 400 seconds were discarded in postprocessing to avoid transient effects.

## RESULTS

### Damping level of the monopile with and without TMD

A unidirectional TMD is considered that acts in the  $y$ -direction. The mass and damping of the TMD are tuned such that the effect during the decay test is desirable. This is an iterative process. Figure 6 shows the time series of the decay test for the final optimal TMD, whose mass amounts to approximately 2% of the monopile support structure's mass. Peaks from the decay test can be fitted to obtain the damping level. Without the TMD, the damping ratio of the monopile support structure is approximately 1.3%, whereas with the TMD, this damping ratio

has been increased to 7.0%. Figure 7 shows the response spectrum of the decay test after a Fast Fourier Transform [Newland]. As shown, with the TMD, the peak around the first eigenfrequency (0.56 Hz) of the monopile without the rotor-nacelle assembly has been significantly reduced. This indicates that the monopile structure will have reduced resonant motions when the external load frequencies are near the first eigenfrequency.

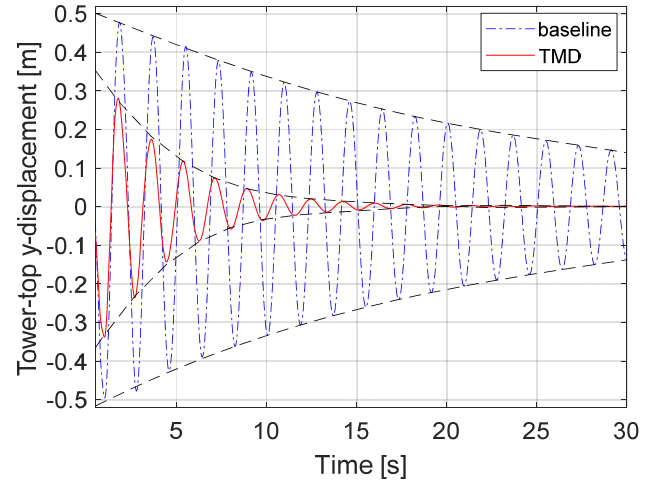


Figure 6 Time series of the tower-top  $y$ -displacement during the decay tests

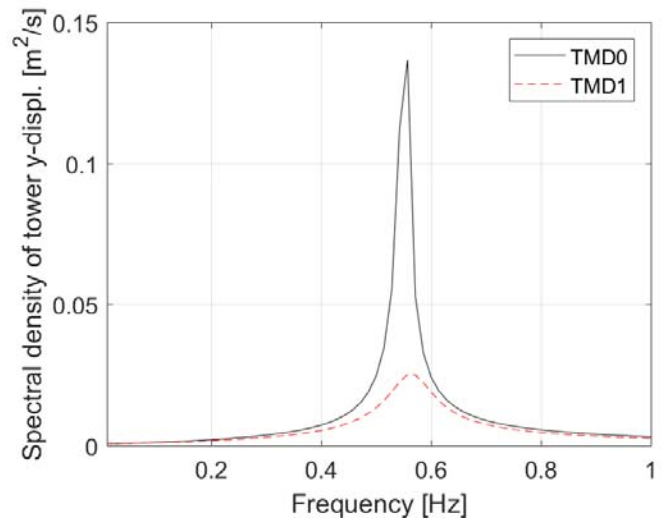


Figure 7 Spectrum of the tower-top  $y$ -displacement during the decay tests

### Time series and spectral analysis

Selected results of LCs 2-4 are presented in the following. Here, TMD0 denotes the monopile structure without TMD, while TMD1 denotes the structure with the TMD. Figure 8 shows a top view of the horizontal displacements of the tower top. As the waves only propagate in the  $y$ -direction with no spreading, wave excitations only exist in the  $x$ -direction, and the tower-top motion in the  $y$ -direction is dominant. With TMD,

the displacement range is substantially reduced for this environmental condition. As the wave peak period equals 4 s and is in the vicinity of the first eigenfrequency of the monopile, the effect of TMD is pronounced as expected. With the TMD, the reduction in the maximum values of the  $y$ -displacement can be more than 100%; see Figure 9. Notice that the maximum value only gives an indication of the TMD effect. For the mating process, the outcrossing rate of two parts will play a more important role; see [11].

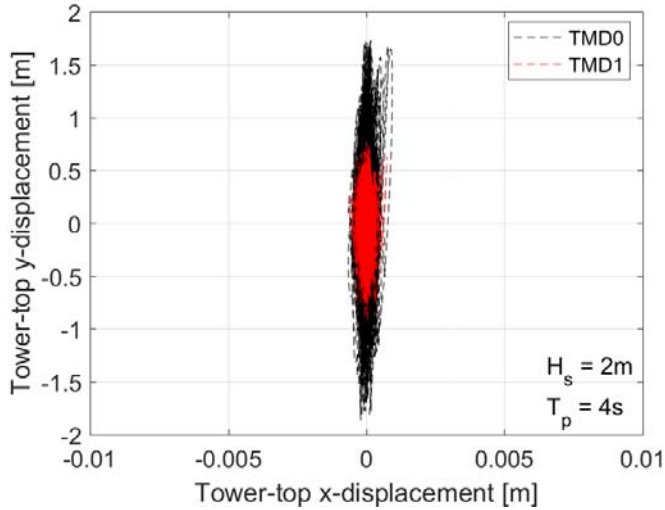


Figure 8 Displacement of the tower-top center in the  $xy$ -plane,  $U_w=12$  m/s,  $H_s=2$  m,  $T_p=4$  s, Seed 1.

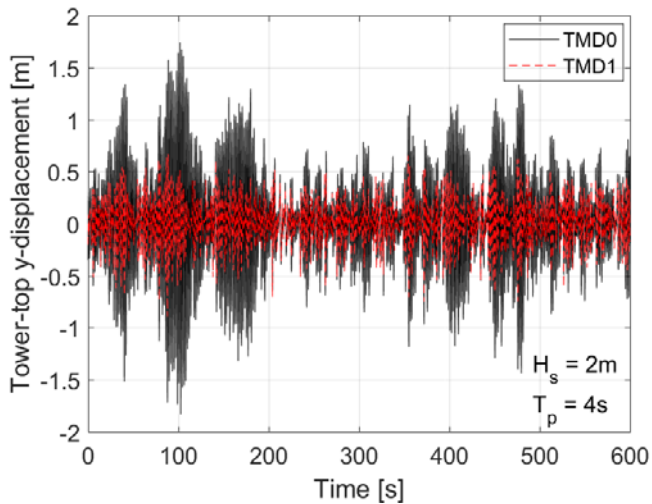


Figure 9 Time series of the tower-top  $y$ -displacement with and without TMD,  $U_w=12$  m/s,  $H_s=2$  m,  $T_p=4$  s, Seed 1.

The response spectra of the tower-top  $y$ -displacement with and without TMD in two sea states are compared in Figure 10 and Figure 11. For the sea state with  $T_p=4$  s, the response is dominated by resonant responses near the first eigenfrequency, and the TMD reduce the spectral peak significantly, as shown by the red dashed line. For the sea state with  $T_p=12$  s, the spectral density has considerably smaller magnitudes as the wave frequencies are far from the first eigenfrequency and limited energy is transferred to the monopile motions. Still, the

spectral peak corresponding to the eigenfrequency ( $f_{FA}$ ) is reduced by the TMD whereas the wave frequency response is not affected. Such an observation is like that of a monopile-nacelle assembly prior to blade mating [11].

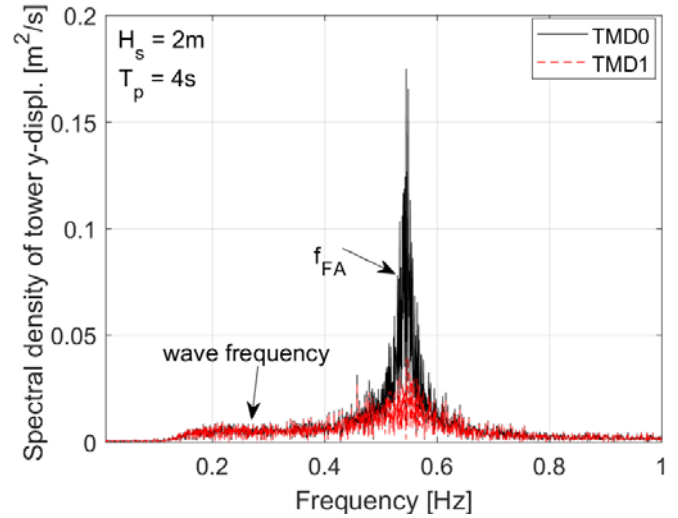


Figure 10 Spectrum of the tower-top  $y$ -displacement with and without TMD,  $U_w=12$  m/s,  $H_s=2$  m,  $T_p=4$  s, Seed 1.

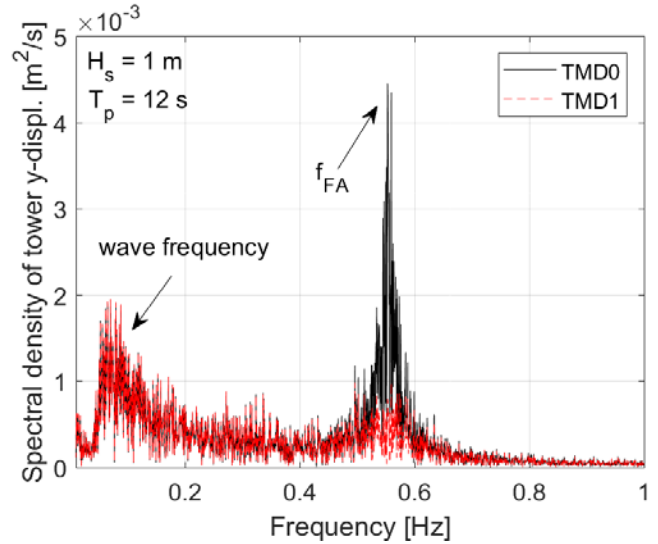
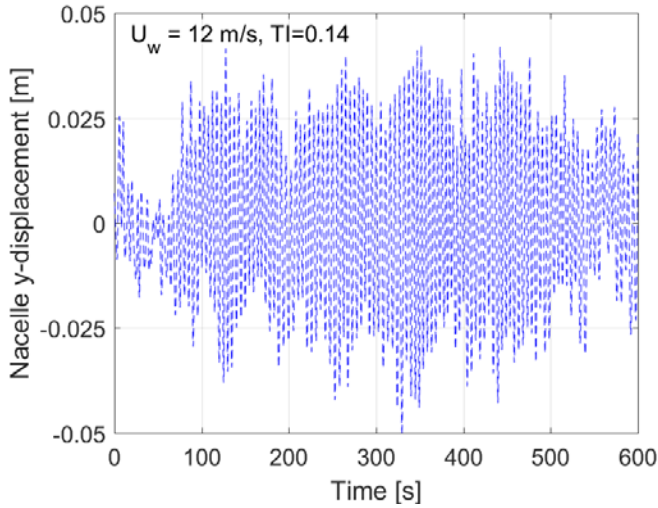
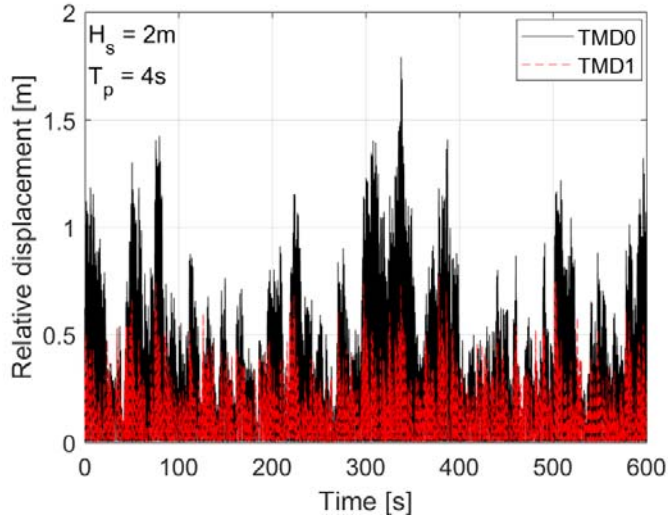


Figure 11 Spectrum of the tower-top  $y$ -displacement with and without TMD,  $U_w=12$  m/s,  $H_s=1$  m,  $T_p=12$  s, Seed 1.



**Figure 12** Time series of the nacelle center  $y$ -displacement,  $U_w=12$  m/s,  $TI=0.14$ ,  $H_s=2$  m,  $T_p=4$  s, Seed 1 (TMD has no effect).



**Figure 13** Time series of the relative distance between nacelle and tower top,  $U_w=12$  m/s,  $TI=0.14$ ,  $H_s=2$  m,  $T_p=4$  s, Seed 1.

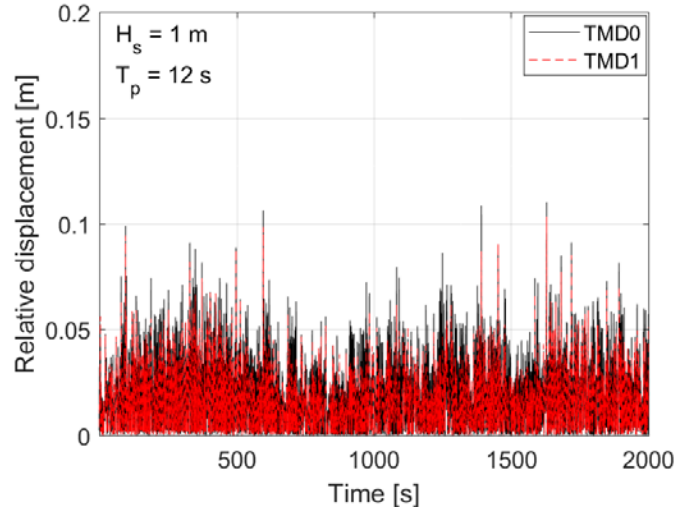


**Figure 14** Time series of the relative distance between nacelle and tower top,  $U_w=12$  m/s,  $TI=0.14$ ,  $H_s=1$  m,  $T_p=12$  s, Seed 1.

Figure 12 shows a time series of the nacelle displacement in the wind direction. Because the crane ends are rigidly fixed, wave loads are assumed to have no influence on the nacelle responses. Although the mean wind speed and turbulence intensity are close to the operating limits of 11 m/s for offshore installation, the nacelle displacements are quite limited with the maximum value less than 0.05 m during the 600-s simulation. This can be explained by two reasons. First, the nacelle subsystem has relatively short tugger lines that constrain the nacelle's pendulum motion. Second, the nacelle has quite large inertia because of its weight. From Figure 12, it is expected that the tower-top motion is dominant when the relative displacement between the nacelle and the tower top is concerned.

As shown in Figure 13 and Figure 14, the effect of TMD on the relative motion varies significantly for different sea states. When  $T_p$  is in the vicinity of the monopile natural period  $t_{FA1}$ , the relative displacement is large because of the monopile resonant motion, and the TMD can effectively reduce the relative displacement. As  $T_p$  gets away from the monopile natural period, the relative displacement is small and the TMD effect becomes insignificant.

### Response statistics of tower-top and nacelle motions

For an offshore mating process, both relative displacement and relative velocity between the two parts can be important. Large relative displacement can cause misalignment of the guide pin on the nacelle and the flange hole on the tower, whereas excessive relative velocity can cause damage of the guide pin due to impact. The latter could further lead to delay of installation tasks [9]. In this section, the effect of the TMD will be evaluated based on statistical average of the nacelle, tower top, and their relative motions.

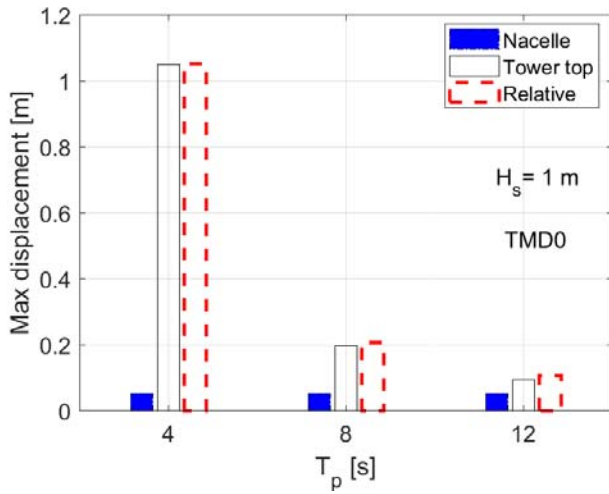


Figure 15 Comparison of maximum displacements without TMD,  $U_w=12$  m/s,  $H_s=1$  m, averaged by 6 simulations

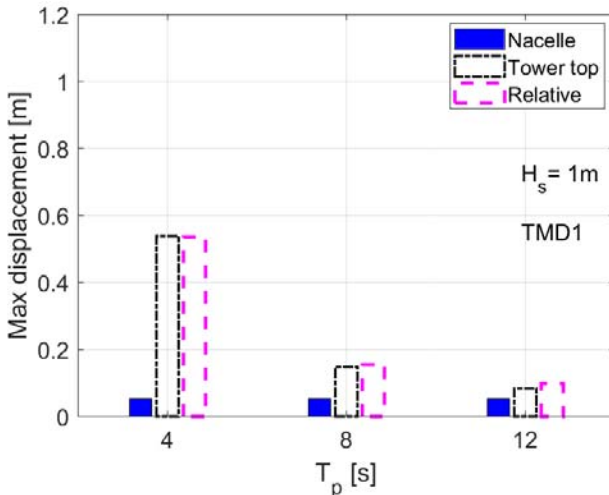


Figure 16 Comparison of maximum displacements with TMD,  $U_w=12$  m/s,  $H_s=1$  m, averaged by 6 simulations

Figure 15 and Figure 16 present the maximum displacement under three different  $T_p$  without and with TMD, respectively. As shown, the 600-s maximum displacement is very sensitive to  $T_p$ . At  $T_p=4$  s, the TMD reduces the maximum displacement to 0.55 m by more than 50%. Despite this reduction, it can still be challenging to mate the nacelle and the tower top under such a sea state. The percentage reduction drops for higher  $T_p$ . As the nacelle displacement is negligible compared to the tower-top displacement, the maxima of the relative displacement and tower-top displacement are on the same level.

The trend of the maximum velocity of the nacelle, tower top, and relative motion is analogous to that of the maximum displacement. As illustrated in Figure 17, under a sea state of  $H_s=1$  m and  $T_p=4$  s, both the maximum tower-top velocity and relative velocity approach 4 m/s. For  $T_p=8$  s, this magnitude reduces to approximately 0.8 m/s. If the TMD is used during

nacelle mating, the maximum relative velocity still reaches 2 m/s for  $T_p=4$  s and 0.4 m/s for  $T_p=8$  s; see Figure 18. This observation indicates that guide pin damage could occur with the TMD for certain sea states, but the weather window for installation can be expanded towards the low  $T_p$  region. The actual weather window depends on the safety criteria and response-based analysis as demonstrated in [8]. This is, however, not further pursued in this paper.

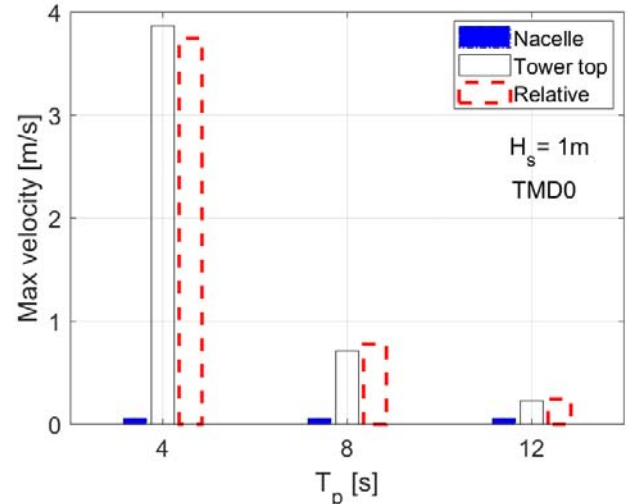


Figure 17 Comparison of maximum velocities without TMD,  $U_w=12$  m/s,  $H_s=1$  m, averaged by 6 simulations

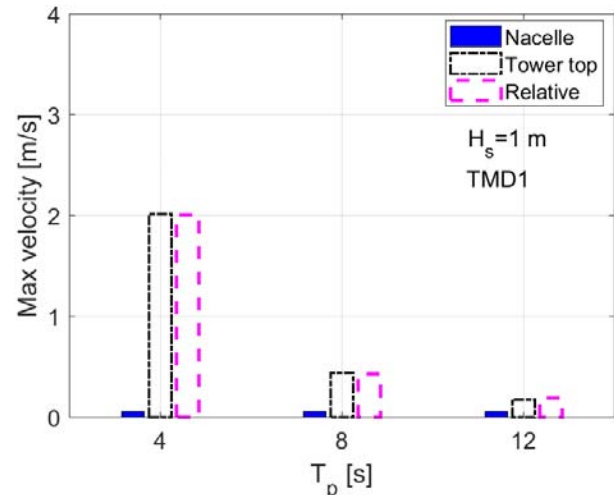


Figure 18 Comparison of maximum velocities with TMD,  $U_w=12$  m/s,  $H_s=1$  m, averaged by 6 simulations

## CONCLUSIONS

In this paper, a numerical study is carried out to investigate the effect of a passive tuned mass damper on the offshore installation process of a nacelle. A nacelle with lifting cables and a monopile of a 10-MW wind turbine, with and without the tuned mass damper, are modelled using the multibody formulation. From dynamic response analysis of the two subsystems in the time domain, the following conclusions are drawn:

- For the considered installation system and process, the wave-induced monopile motions appear to be more significant than the wind-induced nacelle motions, and the relative motion is dominated by the monopile motion.
- The tuned mass damper can reduce the maximum tower-top displacement and the relative displacement between nacelle and tower top by approximately 50% when the spectral peak periods are close to 4 s. Still, for such small peak periods, it would be challenging to perform offshore mating at a significant wave height of 1 m, considering the large relative displacement.
- The actual mating process is more complicated than the one presented by the simplified numerical model. In future, refined numerical models including the crane flexibility can be considered. It is also interesting to investigate other innovative damping systems [20] and their potential applications to offshore wind turbine installation.

## ACKNOWLEDGEMENT

The authors appreciate the contributions from Sander Søvik and Lars Marcussen during their bachelor thesis work at the University of Agder.

## REFERENCES

- [1] Walsh, C.E., *Offshore wind in Europe key trends and statistics 2018*. 2018, Wind Europe.
- [2] Kaiser, M.J. and Snyder, B., *Offshore wind energy installation and decommissioning cost estimation in the US outer continental shelf*. US Bureau of Ocean Energy Management, Enforcement and Regulation, 2010.
- [3] Jiang, Z., Li, L., Gao, Z., Halse, K.H. and Sandvik, P.C., *Dynamic response analysis of a catamaran installation vessel during the positioning of a wind turbine assembly onto a spar platform*. Marine Structures, 2018. **61**: p. 1-24.
- [4] Acero, W.G., Li, L., Gao, Z. and Moan, T., *Methodology for assessment of the operational limits and operability of marine operations*. Ocean Engineering, 2016. **125**: p. 308-327.
- [5] Sarkar, A. and Gudmestad, O.T., *Study on a new method for installing a monopile and a fully integrated offshore wind turbine structure*. Marine Structures, 2013. **33**: p. 160-187.
- [6] Ren, Z., Jiang, Z., Gao, Z. and Skjetne, R., *Active tugger line force control for single blade installation*. Wind Energy, 2017. **21**(12): p.1344-1358.
- [7] Jiang, Z., Gao, Z., Ren, Z., Li, Y. and Duan, L., *A parametric study on the final blade installation process for monopile wind turbines under rough environmental conditions*. Engineering Structures, 2018. **172**: p. 1042-1056.
- [8] Verma, A.S., Jiang, Z., Ren, Z., Gao, Z. and Vedvik, N.P., *Response-Based Assessment of Operational Limits for Mating Blades on Monopile-Type Offshore Wind Turbines*. Energies, 2019. **12**(10): p. 1867.
- [9] Verma, A.S., Jiang, Z., Vedvik, N.P., Gao, Z. and Ren, Z., *Impact assessment of a wind turbine blade root during an offshore mating process*. Engineering Structures, 2019. **180**: p. 205-222.
- [10] Shirzadeh, R., Devriendt, C., Bidakhvidi, M.A. and Guillaume, P., *Experimental and computational damping estimation of an offshore wind turbine on a monopile foundation*. Journal of Wind Engineering and Industrial Aerodynamics, 2013. **120**: p. 96-106.
- [11] Jiang, Z., *The impact of a passive tuned mass damper on offshore single-blade installation*. Journal of Wind Engineering and Industrial Aerodynamics, 2018. **176**: p. 65-77.
- [12] Shabana, A.A., *Dynamics of multibody systems*. 2013: Cambridge University Press.
- [13] Larsen, T.J., *How 2 HAWC2, The User's Manual*. 2009, Risø National Laboratory, Technical University of Denmark: Roskilde, Denmark.
- [14] La Cava, W. and Lackner, M.A., *Theory manual for the tuned mass damper module in FAST v8*. University of Massachusetts Amherst: Amherst, MA, USA, 2015.
- [15] Hoerner, S.F., *Fluid-Dynamic Drag*. Midland Park, NJ, 1965: p. 3-19.
- [16] Faltinsen, O.M., *Sea loads on ships and offshore structures*. Vol. 1. 1993: Cambridge University Press.
- [17] Bak, C., Zahle, F., Bitsche, R., Kim, T., Yde, A., Henriksen, L.C., Hansen, M.H., Blasques, J.P.A.A, Gaunaa, M. and Natarajan, A., *The DTU 10-MW reference wind turbine*. Sound/visual production (digital), 2013.
- [18] Morris, M. *MHI Vestas Launches the First 10 MW Wind Turbine in History*. 2018, accessed 2019 March 01.
- [19] Velarde, J., *Design of monopile foundations to support the DTU 10 MW offshore wind turbine*, Master thesis, Norwegian University of Science and Technology, 2016.
- [20] Constantinou, M.C., Tsopelas, P., Hammel, W. and Sigaher, A.N., *Toggle-brace-damper seismic energy dissipation systems*. Journal of Structural Engineering, 2001. **127**(2): p. 105-112.